Nanoscale Horizons

ROYAL SOCIETY OF CHEMISTRY

COMMUNICATION

View Article Online
View Journal | View Issue

Cite this: *Nanoscale Horiz.*, 2025, **10**, 158

Received 13th August 2024,
Accepted 8th October 2024

DOI: 10.1039/d4nh00400k

rsc.li/nanoscale-horizons

Full-color peptide-based fluorescent nanomaterials assembled under the control of amino acid doping†

Yuhe Shen,[a] Yulin Sun,[a] Yaoyu Liang,[a] Xiaojian Xu,[a] Rongxin Su,[abc] Yuefei Wang *[ac] and Wei Qi *[abc]

Peptide-based biofluorescents are of great interest due to their controllability and biocompatibility, as well as their potential applications in biomedical imaging and biosensing. Here, we present a simple approach to synthesizing full-color fluorescent nanomaterials with broad-spectrum fluorescence emissions, high optical stability, and long fluorescence lifetimes. By doping amino acids during the enzyme-catalyzed oxidative self-assembly of tyrosine-based peptides, we can precisely control the intermolecular interactions to obtain nanoparticles with fluorescence emission at different wavelengths. The synthesized peptide-based fluorescent nanomaterials with excellent biocompatibility and stable near-infrared fluorescence emission were shown to have potential for bioimaging applications. This research provides new ideas for the development of new bioluminescent materials that are cost-effective, environmentally friendly, and safe for biomedical use.

New concepts

This work reports a simple approach to synthesizing peptide-based bioluminescent agents with broad-spectrum fluorescence emissions, high optical stability, and long fluorescence lifetimes. Inspired by the biosynthesis of natural pigments, we incorporated multiple amino acids in the enzyme-catalyzed oxidative self-assembly of tyrosine-based derivatives for co-oxidation and successfully prepared a series of full-color peptide-based fluorescent nanomaterials. The variable side chains of dopant amino acids can change the reaction pathways, chemical structure, and optical properties of the resulting pigments, resulting in different fluorescence emissions that can be artificially controlled and adjusted. Compared with previous studies, the preparation process of this series of bioluminescent agents is simple and controllable, and they exhibit stable, intense emission, low cytotoxicity, and good biocompatibility, thus offering the possibility of further applications under physiological conditions, such as stable biological imaging. The corresponding structural characterization and molecular simulation further revealed these molecules' possible fluorescence emission mechanisms, providing new insights into the artificial design of biological fluorescent nanomaterials that are cost-effective, environmentally friendly, and safe from scratching.

Fluorescent molecules are substances capable of emitting photons of a different wavelength after absorbing light energy at a specific wavelength.[1,2] They play a crucial role across various disciplines, including life sciences, materials science, and environmental science, and are widely used in biomedical imaging, molecular probes, environmental monitoring, and optoelectronic devices.[3–6] High-sensitivity fluorescence detection techniques allow researchers to investigate cellular and molecular processes in depth, and meanwhile, using fluorescent molecules as markers can visualize and track the functional and structural changes of biomolecules, cells, and tissues in real-time, which plays an important role in the development of life medicine and technology.[7–10] Moreover, fluorescent molecules can be used in environmental monitoring to quickly detect pollutants in water and air, effectively protecting the environment and public health.[11] Optoelectronic devices and laser materials including organic light-emitting diodes (OLEDs), lasers, and displays also rely on the unique optical properties of fluorescent materials.[12–14]

Despite their widespread use, traditional fluorescent molecules such as organic dyes and quantum dots are still significant.[15–17] Traditional dyes often suffer from photobleaching, which leads to a decline in fluorescence signal during long-term observations, affecting the imaging quality. Although quantum dots offer high fluorescence quantum yields, heavy metal elements (such as cadmium) commonly used in their synthesis have potential toxic risks and have adverse effects on biological systems and the environment.[18–20] Furthermore, these traditional materials typically have short fluorescence lifetimes and are susceptible to

[a] *State Key Laboratory of Chemical Engineering, School of Chemical Engineering and Technology, Tianjin University, Tianjin 300072, P. R. China. E-mail: wangyuefei@tju.edu.cn, qiwei@tju.edu.cn*
[b] *Collaborative Innovation Centre of Chemical Science and Engineering (Tianjin), Tianjin 300072, P. R. China*
[c] *Tianjin Key Laboratory of Membrane Science and Desalination Technology, Tianjin University, Tianjin 300072, P. R. China*

† Electronic supplementary information (ESI) available. See DOI: https://doi.org/10.1039/d4nh00400k

interference in complex biological or chemical environments, resulting in poor signal stability and limiting their wide application. Therefore, the demand for developing new bioluminescent molecules with high stability and good biocompatibility is increasing.[21–23]

As subunits of proteins, peptides and their derivatives are among the most promising biomimetic luminescent materials.[24–27] They can self-assemble into diverse supramolecular structures, exhibiting unique physical and chemical properties, which have great potential in the fields of biomedicine and life sciences.[28–34] Due to their outstanding biocompatibility, biological activity, structural tunability, and exceptional self-assembly capabilities, peptide-based fluorescent nanomaterials have shown broad application prospects and attracted widespread attention from researchers.[35–37] However, the current synthesis processes of peptide fluorescent molecules are complex and relatively expensive, which are significant barriers to their commercialization and large-scale application. Reducing the preparation cost, improving synthesis efficiency, exploring alternative materials, and introducing other fluorescent composite nanomaterials have become critical research directions in this field.[38–40]

Here, we employed the strategy of doping diverse free amino acids to artificially regulate the enzyme-catalyzed oxidative self-assembly process of tyrosine-based peptide molecules, and controllably synthesize a series of new fluorescent nanomaterials with full-color fluorescence emission (Fig. 1a). The differences in the structures of the doped molecules enabled the regulation of aromatic stacking, hydrogen bonding, and other interactions during the assembly process, thereby altering the chromophore structures and fluorescence properties of the assembled products. These water-soluble fluorescent molecules not only cover a broad spectral range from blue to red but also exhibit excellent optical stability and long fluorescence lifetimes. Moreover, the bioluminescent agents obtained through the oxidation polymerization of substrates regulated by arginine and other alkyl chain-containing molecules show good biocompatibility and fluorescence emission above 600 nm, highlighting their potential in near-infrared bioimaging applications. This research provides new insights into the design and development of novel fluorescent molecules that are simple, cost-effective, environmentally friendly, and safe.

Results

The development of biomaterials with fluorescent properties is highly anticipated because of their promising applications in biomedicine and biotechnology. We previously reported that tyrosine-containing peptides can be oxidized by polyphenol oxidase, which results in incomplete cyclization and prolonged oxidative polymerization when the N-terminus is protected.[41,42] Considering the possibility of doping and regulation of the slow oxidation process,[43] we hypothesized that the addition of amino acid monomers with different side chain groups and molecular polarity would further alter the intermolecular interactions in solution and affect the optical properties of their self-assembly products (Fig. S1, ESI†). Therefore, we introduced a variety of amino acids in the intermediate stages of the enzymatic oxidation process of N-tyrosine-based peptides to intervene in the molecular structure and synthesis pathway of the reaction process, and successfully obtained a series of amino acid fluorescent pigments (X-FP, X = the three-letter abbreviation of the corresponding amino acid doped in the reaction) by utilizing the unstable

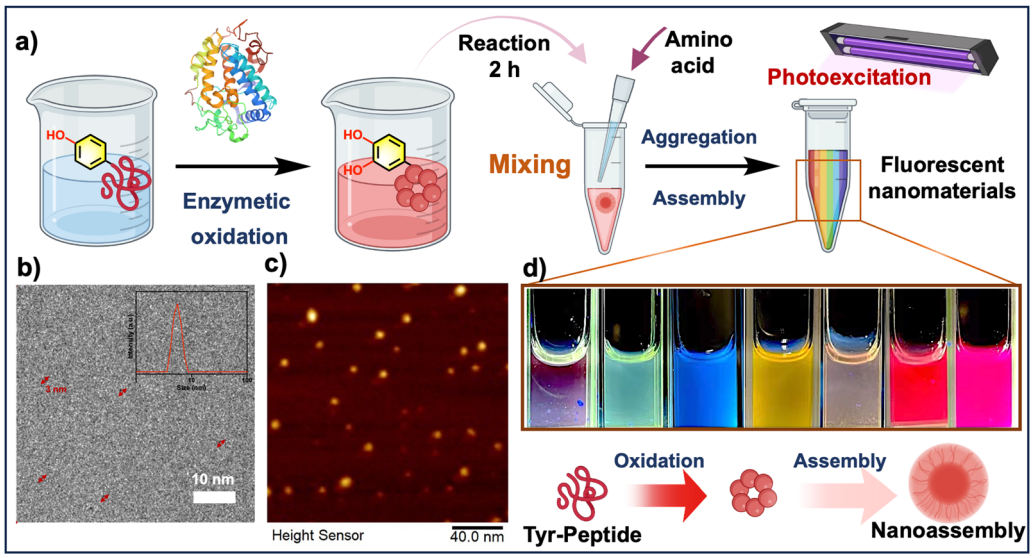

Fig. 1 (a) Schematic diagram of the process of preparing fluorescent nanomaterials by doping amino acids during the enzymatic oxidation of tyrosine-based peptide molecules. (b) Representative cryo-TEM image of self-assembled peptide-based fluorescent nanoparticles (scale bar is 10 nm). The inset shows the particle size distribution of representative fluorescent particles in solution measured by dynamic light scattering (DLS). (c) Representative AFM images of the self-assembled peptide-based fluorescent nanoparticles. (d) Possible oxidative aggregation luminescence process of the Tyr-peptide and fluorescence images of nanoparticle solutions obtained by doping different kinds of amino acids under 365 nm UV light.

state of the intermediates in the reaction process (Fig. 1a). Cryo-transmission electron microscopy (cryo-TEM) and dynamic light scattering (DLS) results confirmed that the resulting self-assemblies were nanoparticles with a particle size of 5–10 nm (Fig. 1b), which is in agreement with the AFM results (Fig. 1c). Under the exposure of 365 nm light, we found that the purified solutions could emit fluorescent emissions with different wavelengths, presenting a variety of fluorescence colors covering the full spectrum (Fig. 1d), which was hypothesized to be a result of the oxidation and polymeric assembly of the peptides that produces aggregation-induced emission (Fig. 2a). To gain a deeper insight into these emission features, the excitation effects of the representative fluorescent nanoparticles prepared here were investigated using photoluminescence (PL) spectroscopy, which showed strong fluorescence emission at different excitation wavelengths (Fig. 2b).

The fluorescence-excitation mapping of 20 biomimetic chromophores further confirmed that the pigment molecules prepared from amino acids with variable side chains displayed strong broad spectrum fluorescence emission completely different from the raw materials (Fig. S2 and S3, ESI†). For instance, different from the fluorescence emission characteristics of phenylalanine residues at about 280–360 nm, Phe-FP solution shows red fluorescence emission at about 580–780 nm. In addition to the common visible light region fluorescence emission, some biomimetic pigment solutions represented by Arg-FP exhibit colorful fluorescence emission at different excitation wavelengths. In particular when the emission wavelength was set around 600 nm, they exhibited strong excitation peaks in the near-infrared fluorescence region, revealing the possibility of their further application in the biomedical field.

To further assess the optical properties of the peptide-based nanoparticles, the time-resolved fluorescence decay kinetics and quantum yields (QYs) of representative fluorescent agents were measured. As shown in Fig. 2c, it revealed that the lifetimes of the assembled pigments Phe-FP, His-FP, and Tyr-FP, which were shown to be red, yellow, and blue–green on the macro scale, were 3.22, 1.93 and 6.29 ns on average at their optimal emission, respectively. The QY of Phe-FP was 24.43%, indicating that the assembled pigment had excellent luminescent properties (Fig. 2d). To assess the photostability of the assembled pigments, we compared them with the green fluorescent organic dyes fluorescein isothiocyanate (FITC) and rhodamine 6G (R6G). After irradiating the pigments under optimal excitation conditions at a rate of one pulse per second for 1000 s, the fluorescence intensity of the Phe-FP remained stable and showed a ~10% reduction at most. In contrast, the

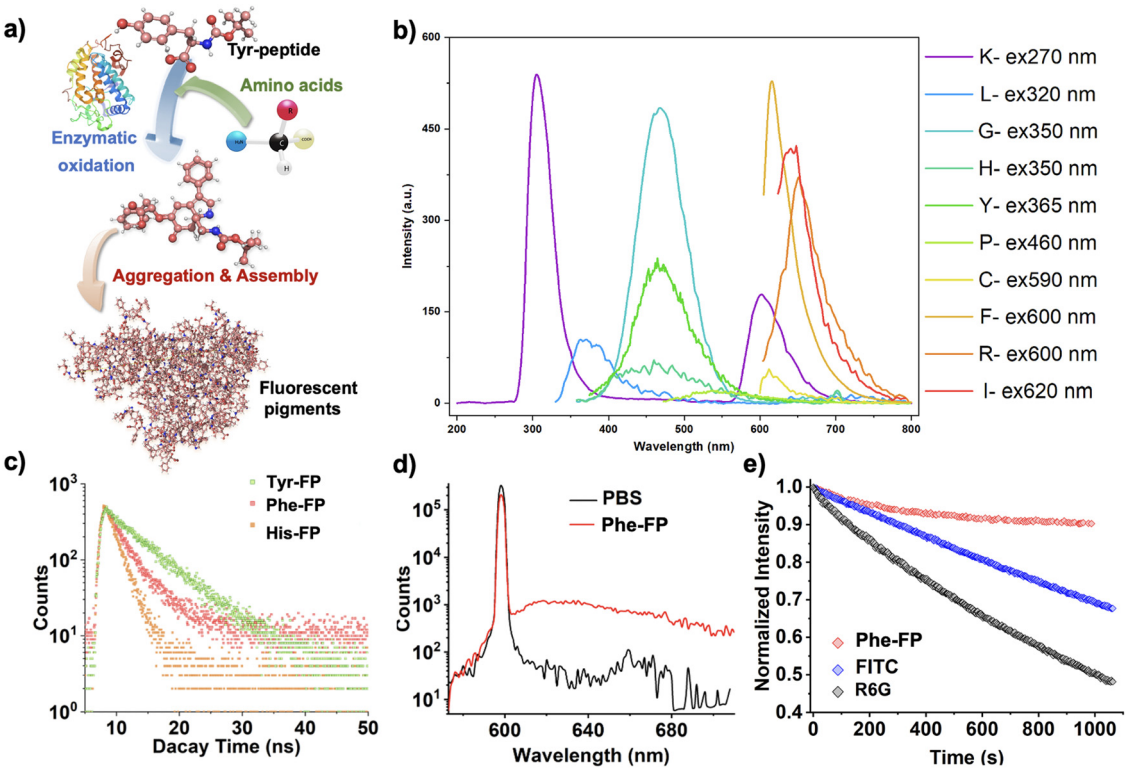

Fig. 2 (a) Schematic diagram of the preparation of fluorescent nanomaterials by doping amino acids during the enzymatic oxidation of tyrosine-based peptide molecules. (b) The emission spectra of representative amino acid-based pigments under their best excitation, showing peaks covering the full spectrum range. (c) Time-resolved emission spectra of the synthesized fluorescent pigments measured in 50 mM phosphate-buffered saline (PBS) solution at a pH of 6.5. (d) Quantum yields (QYs) of the synthesized Phe-FP, determined with the optical absorption set to approximately 0.08 at the optimal excitation wavelength. (e) Evaluation of the photostability of the Phe-FP compared to the organic dyes fluorescein isothiocyanate (FTIC) and rhodamine 6G (R6G). The solutions were subjected to irradiation at a rate of one pulse per second for a total duration of 1000 seconds.

fluorescence intensities of FITC and R6G decreased by around 30% and 54%, respectively, indicating the excellent photostability of the bioluminescent agents (Fig. 2e).

The further application of new bioluminescent agents requires biosafety assessment. Cytotoxicity of the representative fluorescent molecules was measured in HEK293T cells using CCK8 assays as a function of the prepared molecules at doses ranging from 5 to 1000 μg ml^{-1} for 24 hours. Under these conditions, cell viability was maintained at $>80\%$ in all groups, which confirmed that the pigments prepared by this method did not have acute cytotoxicity to HEK293T cells (Fig. 3a). To demonstrate the applicability of the bioluminescent agent for bioimaging, we selected Arg-FP with fluorescence emission above 600 nm (Fig. 3b) and utilized confocal laser scanning microscopy (CLSM) to examine the localization of the respective chromophore. The results, depicted in Fig. 3c, show that after 4 hours of incubation, the Arg-FP exhibited strong red fluorescence in HeLa cells. Additionally, due to the pigment's good photostability and biocompatibility, the fluorescence intensity remained robust even after a 24-hour co-incubation period. Overall, these experiments indicated that the bioluminescent agents prepared in this paper can serve as fluorescent nanoprobes and are promising candidates for cell imaging in both the visible and near-infrared spectra.

In order to further study and understand the assembly and aggregation process of the prepared fluorescent pigments, we calculated the assembly process of Phe-FP monomers using molecular dynamics (MD) methods. Representative snapshots of MD trajectory frames have shown the self-assembly of Phe-FP from monomers to polymers (Fig. 4a). Moreover, we tried to explain the underlying luminescence mechanism of pigment molecules by quantum confinement effects,[44] shallow radiative traps,[45] and electron delocalization.[46] Firstly, the presence of conjugated double bonds and electronic resonances in the

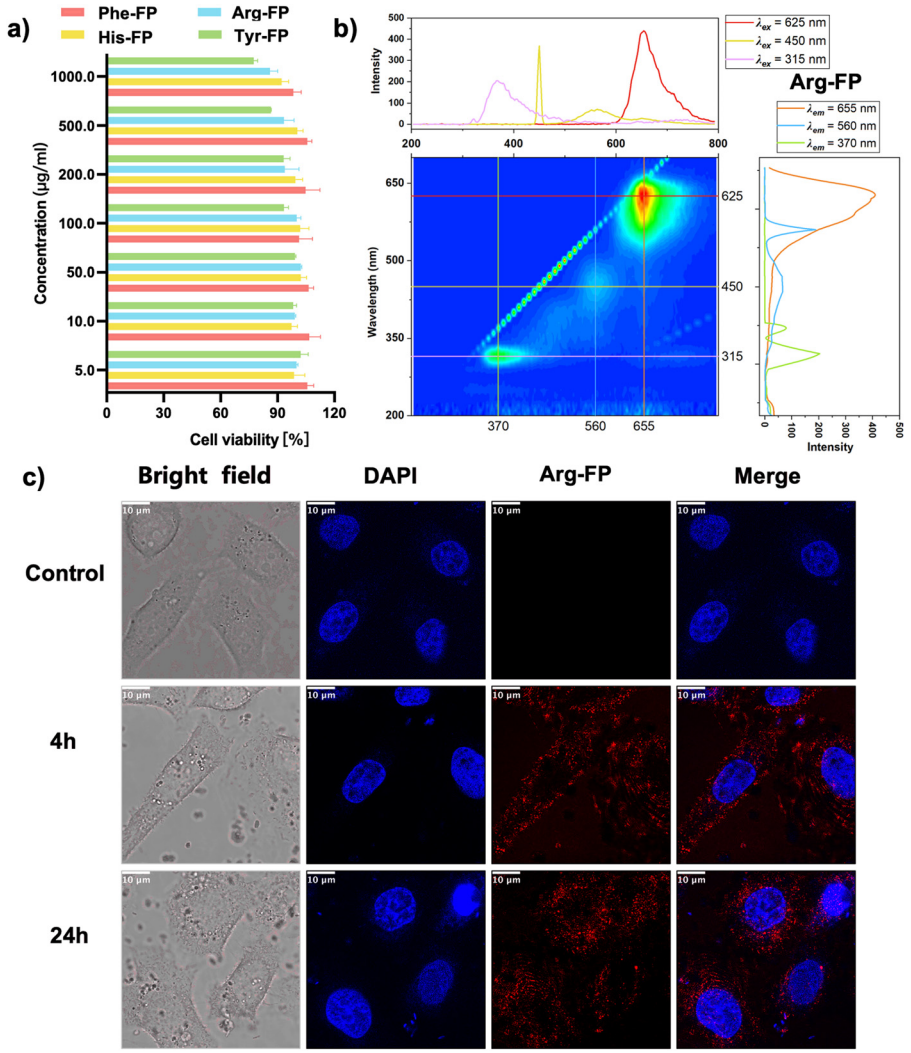

Fig. 3 (a) Results of quantitative biotoxicity measurements on HEK293T cells for 24 h with the representative fluorescent pigment molecules prepared herein. (b) Excitation–emission matrix of the Arg-FP pigment, whose representative excitation and emission spectra are displayed on the top and right projection respectively. (c) *In vitro* fluorescence imaging of HeLa cells treated with selected Arg-FP (100 μg ml^{-1}) for durations ranging from 4 to 24 hours. The red fluorescence signals indicate the presence of pigment within the cells (scale bars: 10 μm).

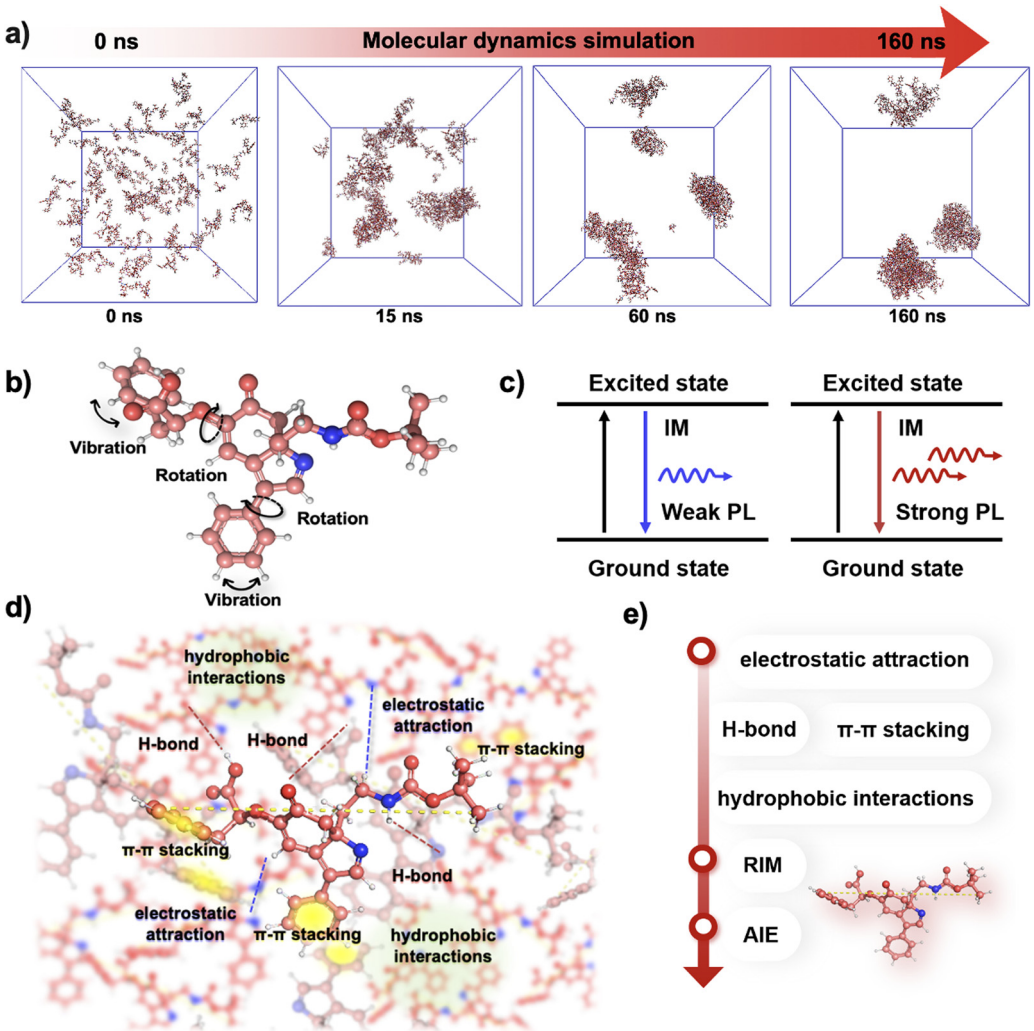

Fig. 4 (a) Snapshots from molecular dynamics (MD) trajectory frames illustrating the assembly and aggregation of Phe-FP monomers. Atoms are color-coded as follows: hydrogen (H) is white, carbon (C) is red, nitrogen (N) is blue, and oxygen (O) is brown. For clarity, water (H_2O) molecules have been excluded from the visual representation. (b) Schematic diagram of Phe-FP molecular structure and internal interactions. (c) Illustration of the restriction of intramolecular motions (RIMs) that contribute to the aggregation-induced emission (AIE) phenomenon. Intermolecular motions (IM) are also depicted. The black arrows pointing upward represent UV absorption, while the downward arrows and red arrows indicate the probability of transition. Nonradiative transitions, attributed to intramolecular motions, result in weak photoluminescence. (d) and (e) The intermolecular interactions between Phe-FP resulted in the restriction of intramolecular motions (RIMs) that in turn led to the aggregation-induced emission (AIE) effect. The red dashed lines denote intermolecular hydrogen bonds, while the blue dashed lines represent electrostatic interactions.

structure of the luminescent monomers endows them with the possibility of fluorescence emission.[47] As shown in Fig. 4b–e, the intense intramolecular motions of the pigment monomers in the solvent before the radiative transition have a large amount of energy consumption, resulting in weak emission.[48] Meanwhile, its further assembly and aggregation (consistent with our previous confirmation by MDs) could form nanosphere structures with strict restriction of intramolecular motions (RIMs), blocking the non-radiative pathway to turn on the fluorescence emission in the visible range.[49] The above experimental and computational simulation results confirm our conjecture that the doping of different amino acids formed multicolored synthetic pigments, which exhibited differentiated optical properties after the oxidation polymerization process regulated by various mechanisms such as ring-opening polymerization and conjugation addition.

Conclusions

In summary, we have successfully developed a method to produce full-color biofluorescents through the pre-organization and self-assembly of tyrosine derivatives doped with various amino acids during controlled enzymatic oxidation. The inclusion of amino acids with different side chains enables the precise modulation of the chemical structure and optical properties of the resulting chromophores, leading to broad-spectrum fluorescence emissions through aggregation-induced emission.

These peptide-based fluorescent nanomaterials demonstrate excellent photostability, high quantum yields, and low cytotoxicity, which highlights the potential of peptide-based fluorescent nanomaterials as versatile and biocompatible tools for advanced biomedical imaging.

Author contributions

Y. W. and Y. S. designed the experiment. Y. S., Y. S. and X. X. performed the experiments. Y. S., Y. W., and R. S. analyzed the experimental data. Y. L. performed the molecular dynamics simulations. Y. S. wrote the manuscript. Y. W. revised the manuscript. Y. W. and W. Q. conceived the project. Yuhe Shen and Yulin Sun contributed equally to this work. All authors approved the final version of the manuscript.

Data availability

The data supporting this article have been included as part of the ESI† and can be found in the online version.

Conflicts of interest

There are no conflicts to declare.

Acknowledgements

This work was supported by the Natural Science Foundation of China (No. 22278314, 22278306, 22078239), the National Key Research and Development Program of China (No. 2019YFE0106900), the Seed Foundation of Tianjin University (No. 2023XJD-0067), and the State Key Laboratory of Chemical Engineering (No. SKL-ChE-22T05).

References

1 J. Querner and T. Wolff, *Angew. Chem., Int. Ed.*, 2002, **41**, 3063–3064.
2 Y. Yang, Q. Zhao, W. Feng and F. Li, *Chem. Rev.*, 2013, **113**, 192–270.
3 A. M. Smith and S. M. Nie, *Acc. Chem. Res.*, 2010, **43**, 190–200.
4 J. Yang, S. W. Chen, B. W. Zhang, Q. Tu, J. Y. Wang and M. S. Yuan, *Talanta*, 2022, **240**, 123200.
5 S. R. Forrest, *Nature*, 2004, **428**, 911–918.
6 G. Y. Wiederschain, *Biochemistry*, 2011, **76**, 1276.
7 K. M. Dean and A. E. Palmer, *Nat. Chem. Biol.*, 2014, **10**, 512–523.
8 Y. W. Yang, Y. Chen, P. Pei, Y. Fan, S. F. Wang, H. X. Zhang, D. Y. Zhao, B. Z. Qian and F. Zhang, *Nat. Nanotechnol.*, 2023, **18**, 1195.
9 D. Wu, L. Chen, W. Lee, G. Ko, J. Yin and J. Yoon, *Coord. Chem. Rev.*, 2018, **354**, 74–97.
10 T. Terai and T. Nagano, *Curr. Opin. Chem. Biol.*, 2008, **12**, 515–521.
11 A. S. Klymchenko, *Acc. Chem. Res.*, 2017, **50**, 366–375.
12 S. Reineke, F. Lindner, G. Schwartz, N. Seidler, K. Walzer, B. Lüssem and K. Leo, *Nature*, 2009, **459**, 234-U116.
13 M. C. Gather, A. Köhnen and K. Meerholz, *Adv. Mater.*, 2011, **23**, 233–248.
14 W. Z. Yuan, Y. Y. Gong, S. M. Chen, X. Y. Shen, J. W. Y. Lam, P. Lu, Y. W. Lu, Z. M. Wan, R. R. Hu, N. Xie, H. S. Kwok, Y. M. Zhang, J. Z. Sun and B. Z. Tang, *Chem. Mater.*, 2012, **24**, 1518–1528.
15 U. Resch-Genger, M. Grabolle, S. Cavaliere-Jaricot, R. Nitschke and T. Nann, *Nat. Methods*, 2008, **5**, 763–775.
16 Q. S. Zheng, A. X. Ayala, I. Chung, A. V. Weigel, A. Ranjan, N. Falco, J. B. Grimm, A. N. Tkachuk, C. Wu, J. Lippincott-Schwartz, R. H. Singer and L. D. Lavis, *ACS Cent. Sci.*, 2019, **5**, 1602–1613.
17 Y. Jung, S. Jeong, W. Nayoun, B. Ahn, J. Kwag, S. G. Kim and S. Kim, *J. Biomed. Opt.*, 2015, **20**(4), 046012.
18 Q. S. Zheng, A. X. Ayala, I. Chung, A. V. Weigel, A. Ranjan, N. Falco, J. B. Grimm, A. N. Tkachuk, C. Wu, J. Lippincott-Schwartz, R. H. Singer and L. D. Lavis, *ACS Cent. Sci.*, 2020, **6**, 1844.
19 M. Ussia, V. Privitera and S. Scalese, *Adv. Mater. Interfaces*, 2024, **11**, 2300970.
20 L. Cui, C. C. Li, B. Tang and C. Y. Zhang, *Analyst*, 2018, **143**, 2469–2478.
21 G. Niu and X. Y. Chen, *Theranostics*, 2012, **2**, 413–423.
22 H. Kobayashi, M. Ogawa, R. Alford, P. L. Choyke and Y. Urano, *Chem. Rev.*, 2010, **110**, 2620–2640.
23 Z. Y. Yang, Z. Mao, Z. L. Xie, Y. Zhang, S. W. Liu, J. Zhao, J. R. Xu, Z. G. Chi and M. P. Aldred, *Chem. Soc. Rev.*, 2017, **46**, 915–1016.
24 J. Kong, Y. Wang, W. Qi, R. Su and Z. He, *ACS Appl. Mater. Interfaces*, 2019, **11**, 15401–15410.
25 J. Kong, J. Zhang, Y. Wang, W. Qi, M. Huang, R. Su and Z. He, *ACS Appl. Mater. Interfaces*, 2020, **12**, 31830–31841.
26 C. L. Walker, K. A. Lukyanov, I. V. Yampolsky, A. S. Mishin, A. S. Bommarius, A. M. Duraj-Thatte, B. Azizi, L. M. Tolbert and K. M. Solntsev, *Curr. Opin. Chem. Biol.*, 2015, **27**, 64–74.
27 Z. Fan, L. Sun, Y. Huang, Y. Wang and M. Zhang, *Nat. Nanotechnol.*, 2016, **11**, 388–394.
28 R. S. Seoudi and A. Mechler, *Pept. Pept. Biomater. Biomed. Appl.*, 2017, **1030**, 51–94.
29 Z. Fan, Y. Chang, C. Cui, L. Sun, D. H. Wang, Z. Pan and M. Zhang, *Nat. Commun.*, 2018, **9**, 2605.
30 R. Riek and D. S. Eisenberg, *Nature*, 2016, **539**, 227–235.
31 H. Wang, Z. Feng and B. Xu, *Chem. Soc. Rev.*, 2017, **46**, 2421–2436.
32 A. Lampel, S. A. McPhee, H. A. Park, G. G. Scott, S. Humagain, D. R. Hekstra, B. Yoo, P. Frederix, T. D. Li, R. R. Abzalimov, S. G. Greenbaum, T. Tuttle, C. Hu, C. J. Bettinger and R. V. Ulijn, *Science*, 2017, **356**, 1064–1068.
33 Y. H. Shen, Y. F. Wang, I. W. Hamley, W. Qi, R. X. Su and Z. M. He, *Prog. Polym. Sci.*, 2021, **123**, 101469.
34 Q. Li, Y. F. Wang, G. Zhang, R. X. Su and W. Qi, *Chem. Soc. Rev.*, 2023, **52**, 1549–1590.
35 O. Berger, L. Adler-Abramovich, M. Levy-Sakin, A. Grunwald, Y. Liebes-Peer, M. Bachar, L. Buzhansky, E. Mossou,

V. T. Forsyth, T. Schwartz, Y. Ebenstein, F. Frolow, L. J. W. Shimon, F. Patolsky and E. Gazit, *Nat. Nanotechnol.*, 2015, **10**, 353–360.
36 Z. Fan, L. M. Sun, Y. J. Huang, Y. Z. Wang and M. J. Zhang, *Nat. Nanotechnol.*, 2016, **11**, 388.
37 E. Gazit, *Nat. Nanotechnol.*, 2016, **11**, 309–310.
38 A. T. Krueger and B. Imperiali, *ChemBioChem*, 2013, **14**, 788–799.
39 F. de Moliner, Z. Konieczna, L. Mendive-Tapia, R. S. Saleeb, K. Morris, J. A. Gonzalez-Vera, T. Kaizuka, S. G. N. Grant, M. H. Horrocks and M. Vendrell, *Angew. Chem., Int. Ed.*, 2023, **62**, e202216231.
40 Z. M. Cheng, E. Kuru, A. Sachdeva and M. Vendrell, *Nat. Rev. Chem.*, 2020, **4**, 275–290.
41 Y. H. Shen, J. Y. Liu, Y. F. Wang, W. Qi, R. X. Su and Z. M. He, *ACS Appl. Mater. Interfaces*, 2021, **13**, 34851–34864.
42 Y. H. Shen, D. S. Jia, Y. F. Wang, T. Yu, X. J. Xu, H. Chang, Q. Li, R. X. Su and W. Qi, *Dyes Pigm.*, 2023, **216**, 111360.
43 Y. H. Shen, R. X. Su, H. Altug, Z. K. Liu, X. L. Zhang, X. J. Xu, Y. Y. Liang, J. Kong, Q. Li, Y. F. Wang and W. Qi, *ACS Appl. Mater. Interfaces*, 2024, **16**(31), 40531–40542, DOI: **10.1021/acsami.4c06070**.
44 J. Kong, Y. F. Wang, W. Qi, R. X. Su and Z. M. He, *ACS Appl. Mater. Interfaces*, 2019, **11**, 15401–15410.
45 T. Nikitin, S. Kopyl, V. Y. Shur, Y. V. Kopelevich and A. L. Kholkin, *Phys. Lett. A*, 2016, **380**, 1658–1662.
46 A. Handelman, N. Kuritz, A. Natan and G. Rosenman, *Langmuir*, 2016, **32**, 2847–2862.
47 Z. X. Gan, M. Meng, Y. S. Di and S. S. Huang, *New J. Chem.*, 2016, **40**, 1970–1973.
48 J. D. Luo, Z. L. Xie, J. W. Y. Lam, L. Cheng, H. Y. Chen, C. F. Qiu, H. S. Kwok, X. W. Zhan, Y. Q. Liu, D. B. Zhu and B. Z. Tang, *Chem. Commun.*, 2001, 1740–1741, DOI: **10.1039/b105159h**.
49 J. Mei, N. L. C. Leung, R. T. K. Kwok, J. W. Y. Lam and B. Z. Tang, *Chem. Rev.*, 2015, **115**, 11718–11940.

